

ChemComm

Accepted Manuscript



This is an *Accepted Manuscript*, which has been through the Royal Society of Chemistry peer review process and has been accepted for publication.

Accepted Manuscripts are published online shortly after acceptance, before technical editing, formatting and proof reading. Using this free service, authors can make their results available to the community, in citable form, before we publish the edited article. We will replace this *Accepted Manuscript* with the edited and formatted *Advance Article* as soon as it is available.

You can find more information about *Accepted Manuscripts* in the [Information for Authors](#).

Please note that technical editing may introduce minor changes to the text and/or graphics, which may alter content. The journal's standard [Terms & Conditions](#) and the [Ethical guidelines](#) still apply. In no event shall the Royal Society of Chemistry be held responsible for any errors or omissions in this *Accepted Manuscript* or any consequences arising from the use of any information it contains.

Cite this: DOI: 10.1039/c0xx00000x

www.rsc.org/chemcomm

COMMUNICATION

DNA-mediated supercharged fluorescent protein/graphene oxide interaction for label-free fluorescent assay of base excision repair enzyme activity†Zhen Wang^{1†}, Yong Li^{1†}, Lijun Li^{1,2}, Daiqi Li¹, Yan Huang^{1*}, Zhou Nie^{1*}, Shouzhao Yao¹

⁵ Received (in XXX, XXX) Xth XXXXXXXXX 20XX, Accepted Xth XXXXXXXXX 20XX
DOI: 10.1039/b000000x

The interaction between supercharged green fluorescent protein (ScGFP) and graphene oxide (GO) as well as the resulting quenching effect of GO to ScGFP were investigated. ¹⁰ Based on this unique quenching effect and the DNA-mediated ScGFP/GO interaction, a label-free fluorescent method has been established for homogeneously assaying the activity and inhibition of base excision repair enzyme.

Biomolecular detection with high sensitivity and selectivity, ¹⁵ simplicity, and low cost is significant in drug discovery, clinical diagnosis, and environmental analysis. Studying interactions between biomolecules and nanomaterials is beneficial for the development of bio-detection methods. Graphene and graphene-like two-dimensional materials attract tremendous interest due to ²⁰ their unusual optical and electronic properties; among them, graphene oxide (GO) is a promising candidate to interact with various biomolecules to build bio-interface for biosensing because of its hydrophilicity, biocompatibility, and ease for bio-functionalization.¹⁻² The unique super-quenching property of GO ²⁵ make GO highly potent as a fluorescent signal transducer, which has been widely exploited in the development of fluorescent nano-sensors.³ However, since most of biomolecules, including proteins and DNA, lack intrinsic fluorescence in the visible region, the GO-based biosensing systems were largely dependent ³⁰ on the fluorophore-labelling biomolecules for signal generation⁴⁻⁷, which requires relatively laborious and costly labelling process. It is still challenging to establish a label-free GO/biomolecule-based fluorescent system.

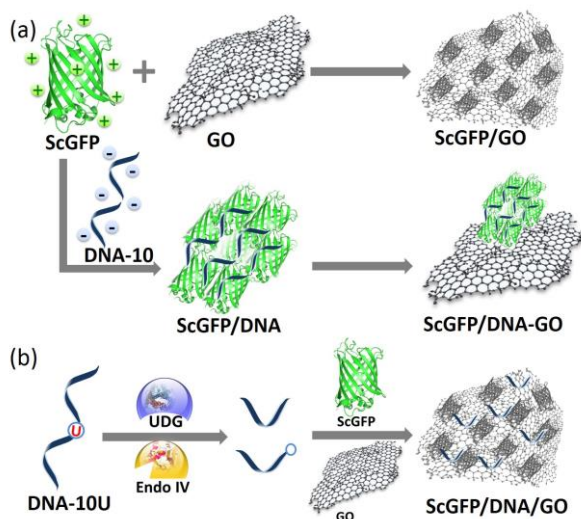
Supercharged proteins are a class of engineered or naturally ³⁵ occurring proteins with unusually strong positive or negative net theoretical charges. Recently, Liu's group developed a new class of supercharged protein, supercharged green fluorescent protein (ScGFP), by extensively mutating surface amino acids of green fluorescent protein (GFP) to basic residues.⁸ With the ⁴⁰ dramatically increased positive net charge on their surface, ScGFPs showed good resistance to self-aggregation, excellent mammalian cell penetration ability, and the capability to highly efficiently deliver functional nucleic acids and proteins into mammalian cell.^{9, 10} Recently, based on the electrostatic ⁴⁵ interaction between DNA and ScGFP, our group developed a versatile biosensing platform for homogenous DNA detection and methylation analysis, indicating the great potential of ScGFP in

bioanalysis.¹¹ Due to its intrinsic fluorescence and highly positively charged protein surface, ScGFP is expected to interact ⁵⁰ with negatively charged GO surface and would be competent to build label-free GO-based biosensor. However, the interaction of ScGFP and nanomaterials is still unexplored. Hence, it is desirable to investigate the interaction between ScGFP and GO for developing novel biosensing mechanisms.

Repair of DNA lesion is of great significance in maintaining ⁵⁵ the integrity of genomes, and refraining the damaged genome from premature ageing, developmental disorders, and/or cancers. There are several specific DNA repair pathways to counteract the deleterious effects of DNA damage, including base excision ⁶⁰ repair (BER), nucleotide excision repair (NER) and mismatch repair (MMR).¹³ BER is the major repair pathway that protects cells from nucleotide base damage and it primarily repairs the damaged base moieties with a relatively small change in the chemical structure. The repair process in BER is initiated by ⁶⁵ specific glycosylases that catalyse the cleavage of the N-glycosidic bond, liberating the damaged base and generating an abasic site (AP site). Then the process is completed by AP endonucleases, deoxyribophosphodiesterases, DNA polymerases, and DNA ligases.¹⁴ Enzymes in BER process is important in ⁷⁰ DNA lesions repair and is connected to both individual and population disease susceptibility, such as lung cancer and bloom syndrome.¹⁵ The assay of BER enzyme activity represents a critical step toward the understanding of DNA damage repairing process, and is significant for the corresponding disease diagnosis.

In this work, the interaction between ScGFP and GO and the ⁷⁵ resulting quenching effect of GO to ScGFP were investigated. Moreover, it was found that DNA can restore the ScGFP fluorescence via mediating the interaction of ScGFP and GO and the DNA ability of restoring fluorescence depends on its ⁸⁰ sequence length. By employing this DNA mediated ScGFP/GO interaction as a new biosensing mechanism, we developed a novel fluorescent sensing system for label-free assay of BER enzyme activity. As shown in Scheme 1 (a), ScGFP readily adsorbs on GO surface, resulting in the highly efficient ⁸⁵ fluorescence quenching of ScGFP. Our previous work revealed that DNA and ScGFP could form a polyionic nano-complex of ScGFP/DNA through electrostatic interaction.¹¹ Here, it was validated that DNA, after forming the ScGFP/DNA nano-complex, could protect ScGFP from being quenched by GO

(Scheme 1a). Interestingly, the protective ability of DNA is sequence length-dependent, which inspired us to design a sensor for DNA lesion-related enzymes assay. In this proof-of-principle study, uracil-DNA glycosylase (UDG) was chosen as a model analyte of DNA BER enzyme. UDG is a highly conserved damage repair protein, which catalyses the cleavage of the N-glycosidic bond between a uracil base and the deoxyribose phosphate backbone of DNA, initiating the BER process to repair the commonly existent damaged uracil base in DNA. Traditional assay methods for UDG enzyme activity mainly focus on the radiometric assay^{16a}, gel-electrophoresis^{16b} and mass spectrometry^{16c}, which suffers from hazardous reagents, expensive labelling, tedious operation, or the requirement of complicated separation or surface immobilization processes. In this work, UDG removes the uracil base from the DNA lesion probe (namely DNA-10U, a 10 nucleotides single-stranded DNA, 10 nt ssDNA, with a U at the fifth nucleotide, and the detailed sequence is shown in ESI) and generates an AP site. Then endonuclease IV (Endo IV) splits off the DNA to two short fragments, which lost the ability to protect ScGFP from being quenched by GO, and resulted in a turn-off fluorescent signal (Scheme 1b). In this way, a simple and quick homogeneous fluorometric assay of DNA UDG enzyme activity was achieved.



Scheme 1 Schematic presentation of ScGFP/GO interaction and DNA-mediated ScGFP-GO interaction (a) and the mechanism of the UDG detection (b).

The ScGFP with +36 theoretical net charge on its surface was prepared by expression in *E.coli* and purified by nickel-affinity chromatography, since it contained a His-tag at its N-terminal. We found that GO (1 $\mu\text{g}/\text{mL}$, detailed characterization shown in Fig. S1) quenched about 97% of ScGFP fluorescence (50 nM) in less than 1 minute at 25 $^{\circ}\text{C}$ (Fig. 1a, Fig. S2 and Fig. S3), and no obvious green fluorescence could be seen by naked eyes when ScGFP/GO were exposed under a 480 nm handheld UV lamp (Fig. 1a, inset). Previous researches indicated that the GO-induced fluorescence quenching originated from fluorescence resonance energy transfer (FRET) between the fluorescent species and GO^{17, 18}. Since the energy transfer is distance-dependent, the high quench efficiency suggested a tight binding between GO and ScGFP, which was proved by AFM results (Fig. S4). Two binding forces might be mainly responsible for this

FRET process: one is the electrostatic interaction between ScGFP and GO; the other is the hydrophobic force induced by ScGFP's His-tag, which enables ScGFP to be adsorbed on GO through π - π interaction between imidazole group and aromatic domains on GO.¹⁹ Herein, eGFP, a kind of GFP with negative net charge (-8) and also His-tag, was used as a control to estimate the contribution of each interaction. The eGFP has similar barrel structure and fluorescence spectrum to ScGFP, and it can also be greatly quenched by GO (Fig. S5b). Since there is a thrombin cleavage site between His-tag and each fluorescent protein, thrombin was exploited to remove His-tag. After thrombin cutting off the His-tag of both fluorescent proteins, the fluorescent intensity of eGFP could be recovered, and increased with increasing amount of thrombin (Fig. S5b), which indicated the His-tag providing the major force for the adsorption of eGFP on GO. Meanwhile, ScGFP kept the same quenching state whether thrombin existed or not (Fig. S5a), which suggested that, despite the His-tag caused π - π interaction, the electrostatic attraction was strong enough for the ScGFP/GO binding.

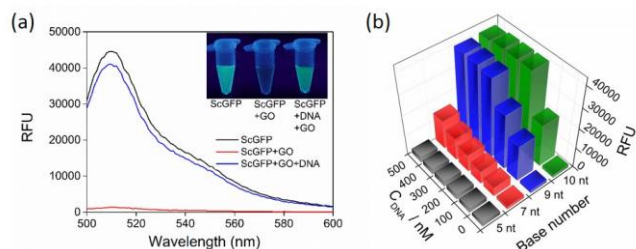


Fig. 1 (a) Fluorescence spectra of ScGFP and its mixture with DNA, GO, and DNA/GO, respectively (DNA used here is the 10 nt ssDNA of DNA-10). Inset is the photo of ScGFP and its mixtures upon excitation at 480 nm under a handheld UV lamp. (b) The influence of the length and the concentration of DNA on its protection of ScGFP (50 nM) fluorescence from being quenched by GO (1 $\mu\text{g}/\text{mL}$). DNA with length from 5 nt to 10 nt and concentration from 0 nM to 500 nM were chosen.

Accordingly, weakening the binding force and increasing the distance between ScGFP and GO can prevent ScGFP from being quenched by GO. Our previous report proved that DNA and ScGFP could quickly form a ScGFP/DNA polyionic nano-complex through the strong electrostatic combination⁴. We expected that the pre-formation of ScGFP/DNA polyionic complex might influence the interaction of ScGFP/GO. To test this assumption, ScGFP (50 nM) was premixed with 200 nM 10 nt single-stranded DNA (namely DNA-10, a ssDNA with similar sequence to DNA-10U but without the nucleotide U, detailed sequence shown in ESI), followed by GO addition (1 $\mu\text{g}/\text{mL}$). It presented an apparent fluorescence recovery up to 92% of initial ScGFP fluorescence (Fig. 1a), indicating that DNA was capable of protecting ScGFP from being quenched by GO. Additionally, the detailed examination of DNA protective effect demonstrated that both the DNA length and the concentration codetermined its protective ability (Fig. 1b). Two hundred nanomolar DNA-10 inhibited majority quenching behavior of GO, while 5 nt ssDNA had ineffectual protection of the ScGFP fluorescence even at 500 nM. In contrast, the existence of 200 nM DNA-10 was incapable of protecting the negatively-charged control eGFP from being quenched by GO (Fig. S6), due to no interaction between eGFP and DNA. The effect of possible influential factors of electrostatic interaction, including pH and ionic strength (adjusted by different NaCl concentrations), on the ScGFP/DNA/GO

system was also studied (Fig. S7). The results showed that the phenomena of DNA-mediated fluorescence recovery of ScGFP/GO system were tolerant of the pH change from 6.5 to 9.5 and the NaCl concentration ranging from 50 to 400 mM, which probably relied on the strong electrostatic interaction caused by highly positive-charged ScGFP. The strong electrostatic interaction between ScGFP and DNA caused the formation of ScGFP/DNA nano-complex, which lead to the embedding of most of ScGFP in nano-complex, and the remarkable neutralization of nano-complex surface charge, significantly decreased the accessibility of GO to the vast majority of ScGFP and weakened the interaction between GO and nano-complex (Scheme 1a). This possible mechanism was supported by the dynamic light scattering (DLS) and zeta potential measurement results of ScGFP/DNA samples. The average diameter of ScGFP/DNA nano-complex is about 300 nm (DLS, Fig. S8). The zeta potential of ScGFP/DNA nano-complex is near -3.3 , which is significantly different from that of ScGFP ($+11.6$) (Fig. S9). Additionally, the ScGFP/DNA nano-complex coexisting with GO exhibited stable fluorescent intensity for more than half hour (Fig. S10), reflecting the robust protection of DNA on ScGFP from GO-induced quenching. The unique DNA-mediated fluorescence switch of ScGFP/GO system and its DNA length-dependent property presents a promising mechanism to design novel biosensors.

Taking advantage of the DNA-mediated ScGFP/GO interaction, a label-free fluorescence assay of UDG activity was implemented, and shown in Scheme 1b. In this assay, the lesion-containing DNA was cleaved by UDG together with Endo IV, and the length change of DNA after the cleavage could be determined by the ScGFP/DNA/GO system. Fig. 2a presents that, similar to DNA-10, when DNA-10U was premixed with ScGFP, the fluorescence intensity of ScGFP recovers to 92%, as well as the obvious green color can be detected by naked eyes under UV lamp. Once UDG (1.0 U/mL)/Endo IV (50 U/mL) were added to split off DNA-10U, an obvious fluorescence decrease was observed (Fig. 2a). We defined the fluorescence quenching ratio as $(F_0-F)/F_0$, where F is the fluorescence intensity of ScGFP coexisting with UDG/Endo IV, DNA-10U, and GO, and F_0 is that of ScGFP only. The quenching ratio of ScGFP was changed from 0.08 to 0.94 after UDG added to DNA-10U, causing a signal to background ratio to be about 12 (Fig. 2b). However, there was negligible fluorescence change when the control DNA (DNA-10) was treated with UDG/Endo IV or not (Fig. 2a, 2b). Besides, 50 U/mL Endo IV, which was used in the assay, solo induced negligible fluorescence change (Fig. S11). All these results suggested that the attenuation of fluorescence was resulted from the uracil removal by UDG, and the proposed mechanism was feasible for UDG assay.

In order to quantitatively detect UDG, different concentrations of UDG was tested by our method under pre-optimized conditions. As shown in Fig. 2c, the fluorescence intensity gradually decreases as the concentration of UDG increases from 0 U/mL to 1.5 U/mL, resulting from the destruction of DNA-10U induced by UDG. The relationship between quenching ratio and the UDG concentration was also given in Fig. 2d, and the calibration curve is provided in the inset, demonstrating a good linear correlation ($Y=0.11+6.4X$, $R^2=0.98$)

in the range of UDG concentration from 0.0050 U/mL to 0.10 U/mL, with the limit of detection of 0.0015 U/mL based on 3σ , which exhibits better or comparable performance to other fluorescent²⁰ and colorimetric methods²¹. Additionally, the detection range of UDG in the proposed assay can be tunable by simply varying the concentrations of DNA-10U and ScGFP (Fig. S12-S14). Moreover, the selectivity of the method was evaluated by challenging the proposed assay with other DNA-related enzymes, including DpnI, dam methyltransferase (Dam MTase), and human alkyladenine glycosylase (hAAG). At the concentration of 10 U/mL, tenfold of that of tested UDG (1 U/mL), none of these enzymes could induce observable fluorescence quenching (Fig. S15). Several factors may be attributed to the excellent performance of the UDG detection method. First, the high fluorescence quenching efficiency of GO leads to low background. Second, DNA firmly binding with ScGFP can retain almost all of the fluorescence and yield a high signal-to-background ratio. Third, the specific recognition of UDG cooperating with Endo IV is beneficial for the sensitivity and selectivity.

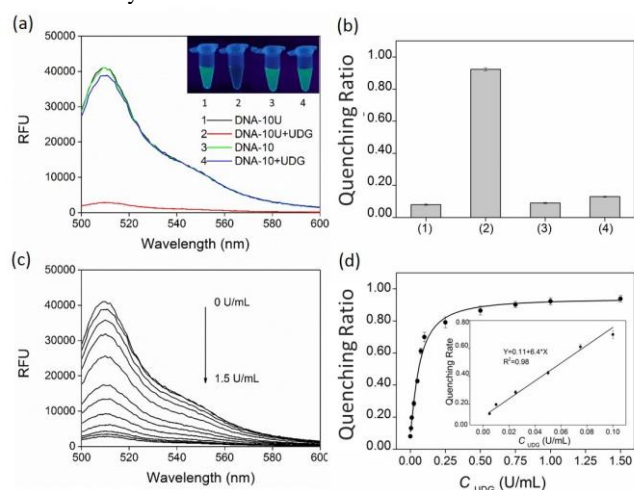


Fig. 2 The fluorescence spectra (a) and the bar graph of quenching ratio (b) of the proposed UDG sensor based on the DNA-mediated ScGFP/GO interaction, and inset in (a) is the fluorescent photograph of the sensor for visualized detection of UDG upon excitation under a handheld UV lamp. ScGFP was mixed with DNA-10U (1), DNA-10U and UDG/Endo IV (2), DNA-10 (3), DNA-10 and UDG/Endo IV (4) before GO addition, respectively. The fluorescence spectra of ScGFP corresponding to the concentration of UDG from 0 - 1.5 U/mL (c) and the calibration curve of quenching ratio as a function of the UDG concentration (d). Inset in (d) shows the linear relationship between quenching ratio and the concentration of UDG.

The feasibility of the method in assaying the inhibition of UDG was also demonstrated, using uracil DNA glycosylase inhibitor (UGI) as a model inhibitor. UGI, which is produced by bacteriophage PBS1, can form an extremely specific and exclusively stable complex with UDG through a 1:1 stoichiometry²². As shown in Fig. 3a, when UDG was mixed with equal amount of UGI (0.050 U/mL or 0.50 U/mL), its activity was completely inhibited, which is perfectly accordant with the reported stoichiometry²². These results replied that the proposed method can be used to monitor the UDG inhibition, and may be potential for further UDG-related inhibitor screening. In addition, the robustness and reproducibility of the proposed method was

evaluated and Z' factor, an available criteria to quantify the suitability of a particular assay for use in a full-scale and high-throughput screen (HTS),²³ was calculated (the equation for calculating Z' factor is shown in ESI). In general, the acceptable value of Z' factor should be between 0.5 and 1 for HTS, as assays with a Z' factor in this range exhibits large dynamic ranges and wide separation of positive and negative results. Fig. 3b and Fig. S16 depict that our method has a robust reproducibility for at least 30 times parallel tests, and the calculated Z' factor of UDG and UGI are 0.82 and 0.75 respectively, indicating that this method was a solid strategy for HTS assays in practice. Hence, our method not only can be applied for simple, rapid and sensitive detection of UDG activity and its inhibition, but also holds the potential of HTS assay in practice.

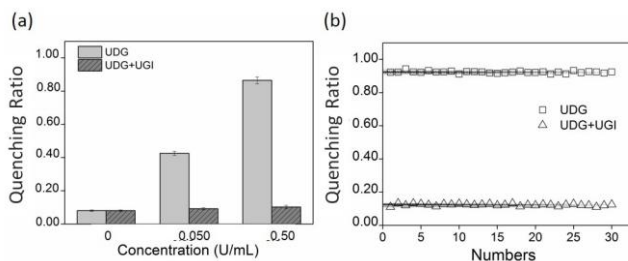


Fig. 3 The bar graph of the quenching ratio of ScGFP when the proposed sensor was mixed with different concentrations of UDG (light column) or UDG coexisting with UGI (with the same concentration as UDG, dark column) (a) and the quenching ratio of ScGFP in 30 times parallel tests by the proposed sensor mixed with UDG (1.0 U/mL) or UDG coexisting with UGI (1.0 U/mL) (b).

In summary, we reported the high efficient quenching of ScGFP by GO and the sequence length-dependent protective effect of DNA against GO-caused ScGFP quenching, and developed a fluorescent biosensing system based on this unique DNA-mediated ScGFP/GO interaction. Based on this system, a label-free and homogenous assay for UDG activity and its inhibition was established. The high quenching ratio of ScGFP/GO and the specific recognition of UDG on DNA lesion give this UDG assay method good sensitivity and selectivity. Meanwhile, compared to other UDG assays requiring radioactive or dye labeling, our method demonstrates several practical advantages, including label-free, facile, cost-effective, and mix-and-read operation. Our method presents a potential platform for high throughput screening assay of BER-targeted anti-cancer drug candidates in pharmaceutical development. Furthermore, this system is versatile and can be expanded to monitor other DNA-related enzymes *in vitro*. This work also revealed that the interaction of ScGFP with nanomaterials might be a promising toolkit to develop new biosensing mechanisms.

This work was funded by the 973 Program (No 2011CB911002), the NSFC (Nos. 21475037, 21190044, 21222507, and 21175036), the Foundation for Innovative Research Groups of NSFC (Grant 21221003), and the fundamental research funds for the central universities.

Notes and references

State Key Laboratory of Chemo/Biosensing and Chemometrics, College of Chemistry and Chemical Engineering, Hunan University, Changsha,

- 410082, P. R. China¹, and Shenzhen Institutes of Advanced Technology, Chinese Academy of Science, Shenzhen 518055, P. R. China².
 Fax: +86-731-88821848; Tel: +86-731-88821626; E-mail: huangyan.hnu@gmail.com, niezhou.hnu@gmail.com
[†]Co-first authors: These two authors contributed equally to this work.
 Electronic Supplementary Information (ESI) available: [details of any supplementary information available should be included here]. See DOI: 10.1039/b000000x/
1. E. N. Morales and A. Merkoci, *Adv. Mater.*, 2012, **24**, 3298-3308.
 2. Y. Wang, Z. Li, D. Hu, C. T. Lin, J. Li and Y. Lin, *J. Am. Chem. Soc.*, 2010, **132**, 9274-9276.
 3. Y. Wang, Z. Li, J. Wang, J. Li and Y. Lin, *Trends Biotechnol.*, 2011, **29**, 205-212.
 4. J. Balapanuru, J. X. Yang, S. Xiao, Q. Bao, M. Jahan, L. Polavarapu, J. Wei, Q. H. Xu and K. P. Loh, *Angew. Chem. Int. Ed.*, 2010, **122**, 6699-6703.
 5. L. Wang, J. Zhu, L. Han, L. Jin, C. Zhu, E. Wang and S. Dong, *ACS Nano.*, 2012, **6**, 6659-6666.
 6. J. H. Jung, D. S. Cheon, F. Liu, K. B. Lee and T. S. Seo, *Angew. Chem. Int. Ed.*, 2010, **49**, 5708-5711.
 7. M. Zhang, B. C. Yin, X. F. Wang and B. C. Ye, *Chem. Commun.*, 2011, **47**, 2399-2401.
 8. M. S. Lawrence, K. J. Phillips and D. R. Liu, *J. Am. Chem. Soc.*, 2007, **129**, 10110-10112.
 9. B. R. Mcnaughton, J. J. Cronican and D. B. Tompon and D. R. Liu, *Proc. Natl. Acad. Sci.*, 2009, **106**, 6111-6116.
 10. J. J. Cronican, K. T. Beier, T. N. Davis, J. C. Tseng, W. D. Li, D. B. Thompson, A. F. Shih, E. M. May, C. L. Cepko, A. L. Kung, Q. Zhou and D. R. Liu, *Chem. Biol.*, 2011, **18**, 833-838.
 11. C. Lei, Y. Huang, Z. Nie, J. Hu, L. Li, G. Lu, Y. Han and S. Yao, *Angew. Chem. Int. Ed.*, 2014, **53**, 8358-8362.
 12. J. E. Cleaver, *Nat. Rev. Cancer*, 2005, **5**, 564-573.
 13. T. A. Kunkel and D. A. Erie, *Annu. Rev. Biochem.*, 2005, **74**, 681-710.
 14. S. S. David and S. D. Williams, *Chem. Rev.*, 1998, **98**, 1221-1261;
 15. G. Xu, M. Herzig, V. Rotrekl and C. A. Walter, *Mech. Ageing Dev.*, 2008, **129**, 366-382.
 16. (a) J. Tchou, H. Kasai, S. Shibutani, M. H. Chung, J. Laval, A. P. Grollman, and S. Nishimura, *Proc. Natl. Acad. Sci.*, 1991, **88**, 4690-4694. (b) H. Krokkan, and C. U. Wittwer, *Nucleic Acids Res.*, 1981, **9**, 2599-2613. (c) A. A. Ischenko, and M. K. Saparbaev, *Nature*, 2002, **415**, 183-187.
 17. C. Liu, Z. Wang and H. Jia, *Chem. Commun.*, 2011, **47**, 4661-4663.
 18. H. Dong, W. Gao, F. Yan, F. Ji, H. J. Hu, *Anal. Chem.*, 2010, **82**, 5511-5517.
 19. S. S. Chou, M. De, J. Luo, V. M. Rotello, J. Huang and V. P. Dravid, *J. Am. Chem. Soc.*, 2012, **134**, 16725-16733.
 20. (a) K. Leung, H. He, V. Y. Ma, H. Zhong, D. S. Chan, J. Zhou, J. Mergny, C. Leung and D. Ma, *Chem. Commun.*, 2013, **49**, 5630-5632. (b) D. Hu, Z. Huang, F. Pu, J. Ren, and X. Qu, *Chem. Eur. J.* 2011, **17**, 1635-1641.
 21. X. Liu, M. Chen, T. Hou, X. Wang, S. Liu and F. Li, *Biosens. Bioelectron.*, 2014, **54**, 598-602.
 22. S. E. Bennett and D. W. Mosbaugh, *J. Biol. Chem.*, 1992, **267**, 22512-22521.
 23. J. H. Zhang, T. D. Chung, K. R. Oldenburg, *J. Biomol. Screening*, 1999, **4**, 67-73.